The CATRiNA Deuterated Neutron Detector Array

J. F. Perello, S. Almaraz-Calderon, B. W. Asher, L. T. Baby, N. Gerken, K. Hanselman
Department of Physics, Florida Sate University, Tallahassee, FL, 32306

Introduction

The CATRiNA neutron detector array has been developed at Florida State University (FSU). CATRiNA consists of 16-deuterated-benzene (C_6D_6) liquid scintillators with high efficiency, pulse shape discrimination (PSD) capabilities and a novel pulse-height dependence (Fig.1) that, along with time-of-flight (ToF), allows for extraction of neutron energies [1,2]. The structure of the pulse-height spectrum is due to the anisotropic backscattering of d-n interactions unlike the isotropic nature of p-n, as shown in Fig. 2.

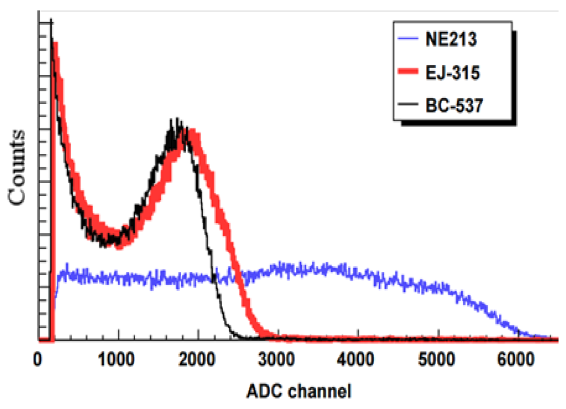

Fig.1: Pulse-Shape spectra of C_6H_6 (NE213) vs C_6D_6 (EJ-315, BC-437) [1].

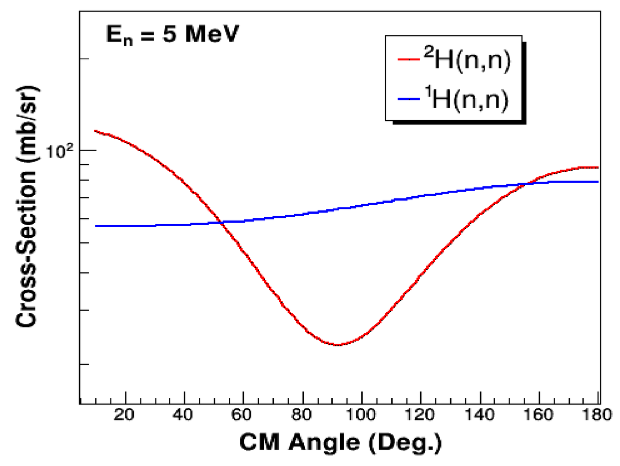

Fig.2: DWBA calculations of d-n and p-n scattering for E_n = 5 MeV.

CATRiNA Detectors

The CATRiNA detectors consist of C_6D_6 scintillating material (EJ-315) [3] contained in a 4" diameter x 2" deep cylinder coupled to a ET Enterprise 9821B PMT [4]. The PMT's anode pulse signal is sent to a MCFD which splits the pulse's timing and amplitude signal components. Two timing and amplitude signals from each detector are sent to independent banks on a MQCD (Fig. 4) for pulse integration. The C_6D_6 detectors are mounted on to a versatile array, where the detector's distance from target can be changed easily to optimize ToF.

Data Acquisition System

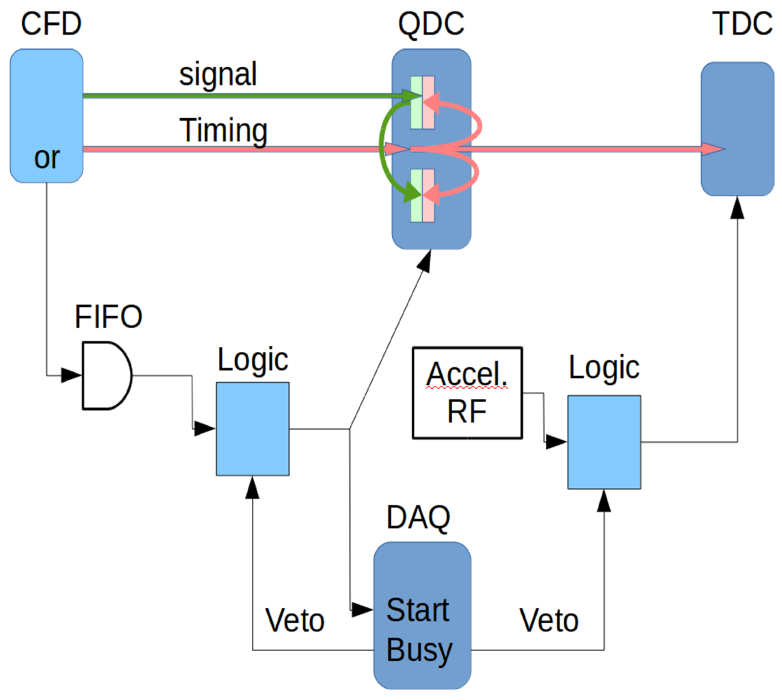

Fig.5: Schematic of CATRiNA's data acquisition system.

Fig.3: One of CATRINA detectors with (left) and without (right) mounting case.

Fig.4: Mesytec QDC.

Simulation & Characterization

Tests with γ/n Sources

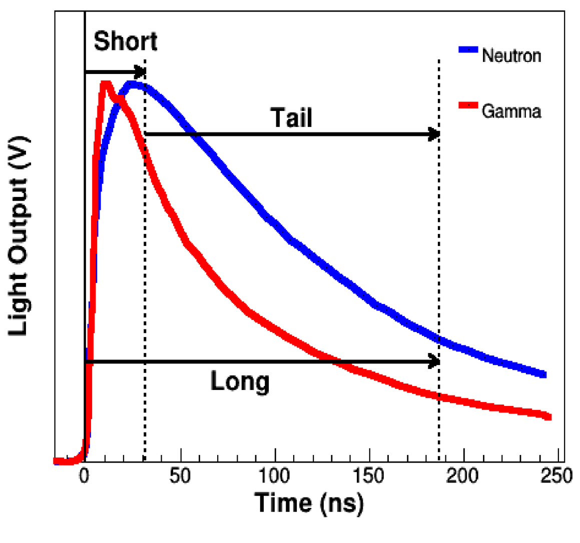

Fig.6: Pulse height signals from interactions of n/γ in the detectors. The different gate integration times are used for PSD.

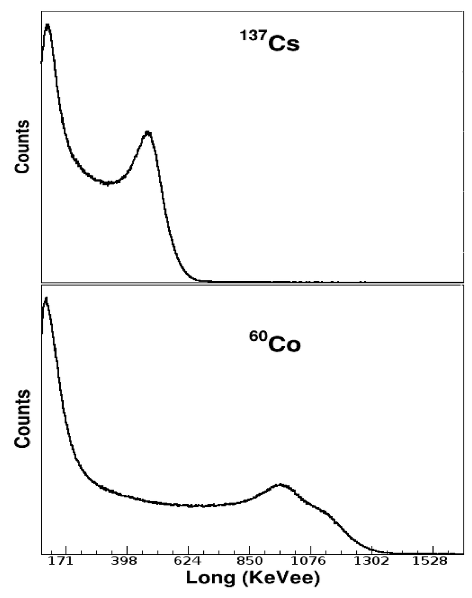

Fig.7: Detector's calibrations. The Compton edges of gamma-ray sources, ^{137}Cs (top), ^{60}Co (bottom) were used to calibrate each detector's QDC spectrum. [5]

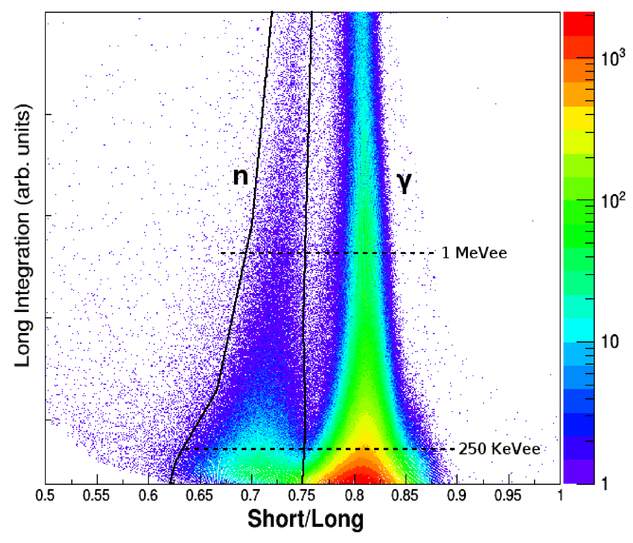

Fig.8: PSD parameters were optimized using a ^{252}Cf source. Here, the long-gate vs ratio short-gate/long-gate shows n/γ separation.

Monte-Carlo Simulations

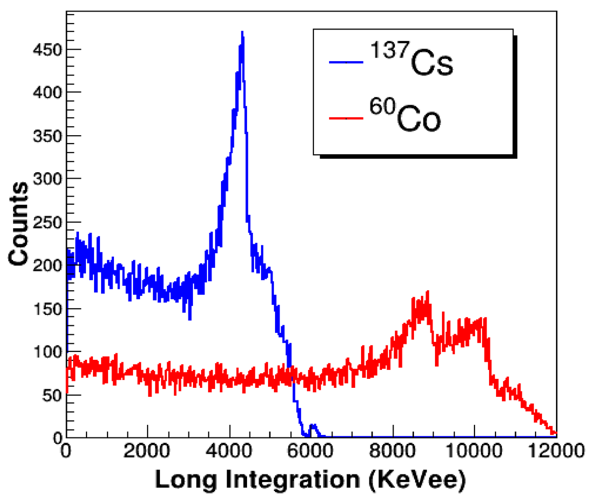

Fig.9: Simulated Compton Edges for ^{60}Co and ^{137}Cs γ-sources on C_6D_6 material using GEANT4.

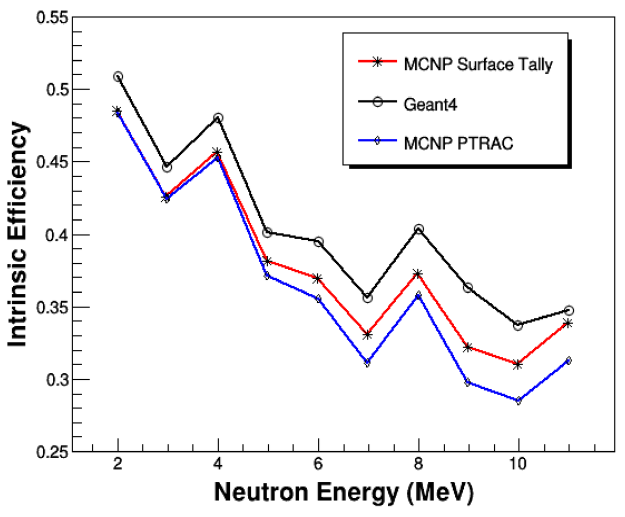

Fig.10: Simulated efficiency curve of mono-energetic neutrons at different energies using GEANT4 and MCNP6's Tally and PTRAC.

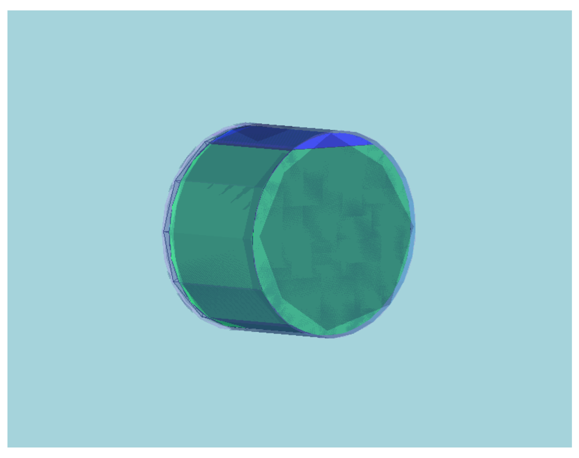

Fig.11: Snapshot of the simulated C_6D_6 material in MCNPX VISED software.

In-Beam Experiments

^{7}Li(p,n)^{7}Be

The ^{7}Li(p,n)^{7}Be reaction was measured to study the response of CATRiNA to mono-energetic neutrons using the FN-Tandem accelerator at the John D. Fox accelerator facility (Fig. 12) at FSU. A proton beam of several energies was used to bombard a LiF target. Quasi-mono-energetic neutrons from the ^{7}Li(p,n_0)^{7}Be reaction were identified via ToF (Fig. 15) and their pulse-shape dependence was compared.

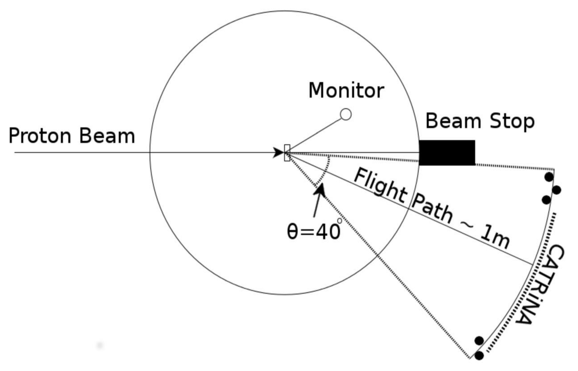

Fig.12: Diagram of experimental setup.

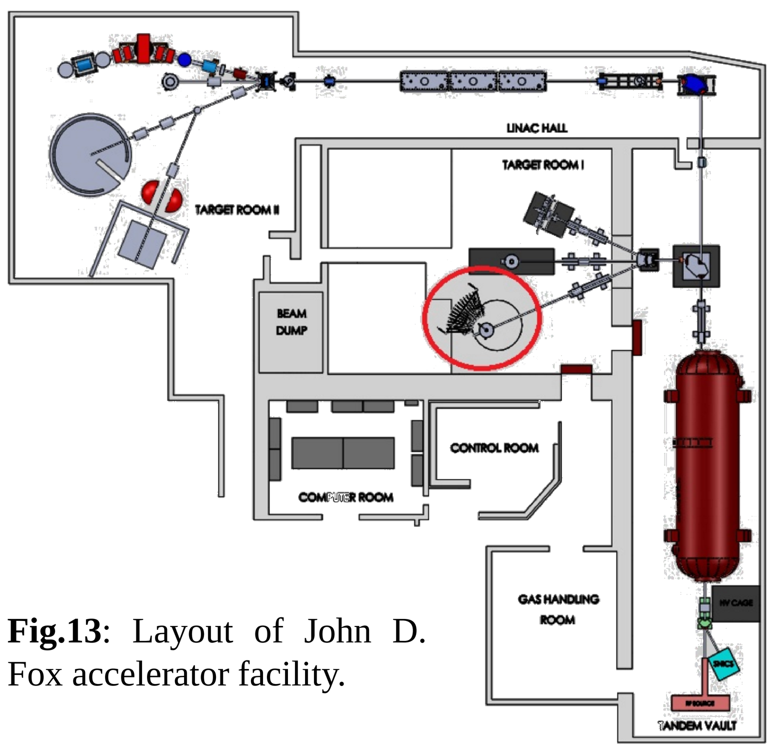

Fig.13: Layout of John D. Fox accelerator facility.

FOM

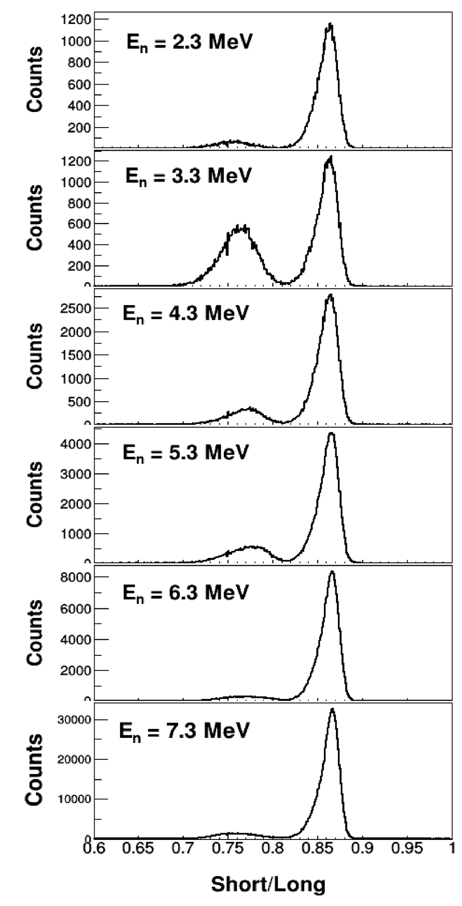

Fig.14: FOM with 250 KeVee threshold. FOM ranged from 1.43 (E_n = 2.3 MeV) to 1.36 (E_n = 7.3 MeV)

n-ToF

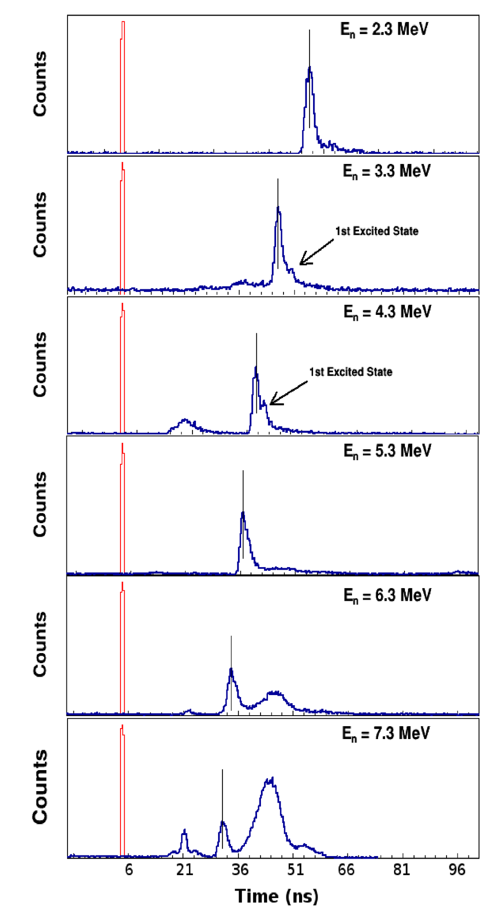

Fig.15: Time-of-Flight spectra of neutrons from the ^{7}Li(p,n) reaction.

n-QDC

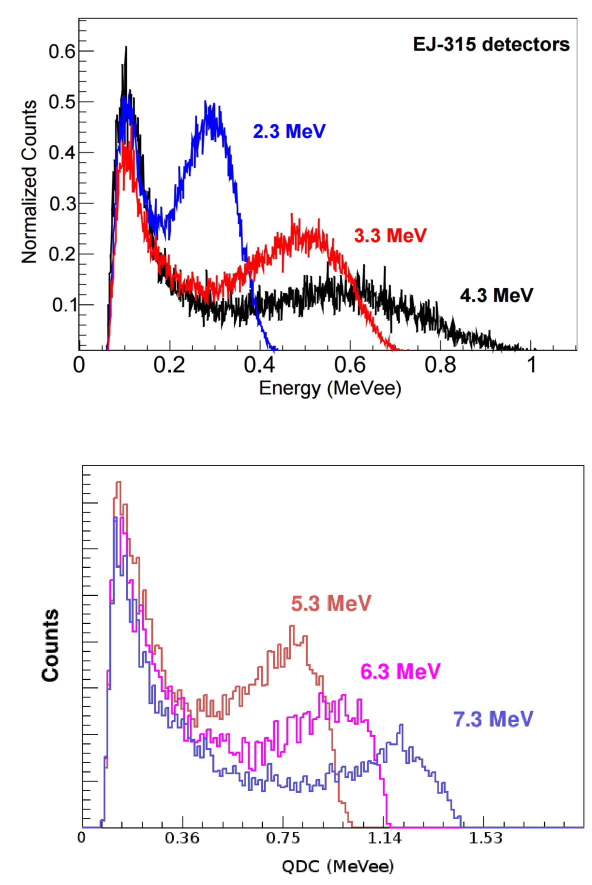

Fig.16: Normalized QDC neutron spectra. The energy dependence of the pulse height is shown as a function of the neutron energy

^{12}C(^{3}He,n)^{14}O

The ^{12}C(^{3}He,n)^{14}O reaction was also studied at FSU using a 3.5 MeV/u bunched ^{3}He beam. Preliminary results of the reaction are shown in Fig. 17, where several resonant states of ^{14}O are observed.

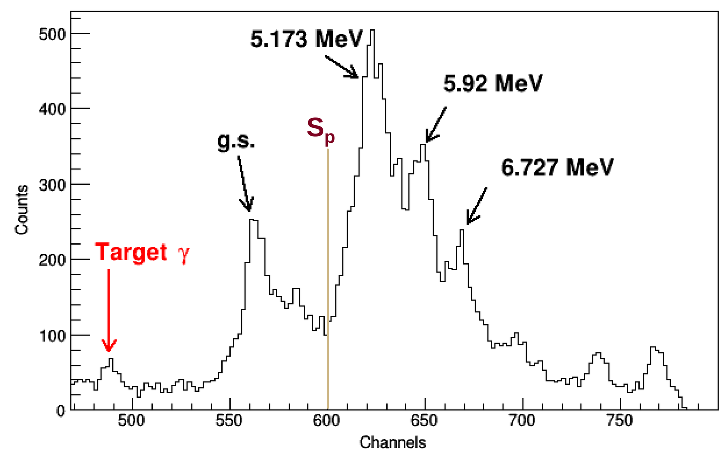

Fig.17: ToF spectrum of the ^{12}C(^{3}He,n)^{14}O reaction.

Future Work

- Measurement of the ^{14}C(d,n) reaction for neutron spectroscopy studies
- Transition to a Digital DAQ
- Coupling to γ-array & silicon detector for coincidence measurements


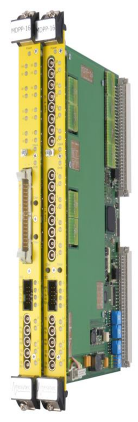
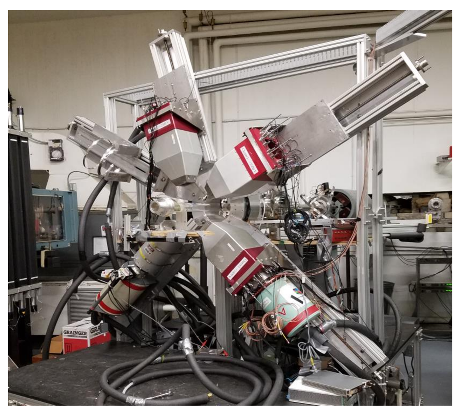

References

[1] V. Bildstein, P.E. Garrett, J. Wong, D. Bandyopadhyay, J. Bangay, L. Bianco, NIM A 729 (2013) 188
[2] M. Febbraro, C.C. Lawrence, H. Zhu, B. Pierson, R.O Torres-Isea, F.D. Becchetti, J.J. Kolata, J. Riggins, NIM A: Volume 784, 2015, P. 184-188, ISSN 0168-9002,
[3] Eljen Technology Deuteratedej315 https://eljentechnology.com/products/liquid-scintillators/ej-315, Accessed: 2018-08-15
[4] ET Enterprises Ltd Photomultipliers http://www.et-enterprises.com/photomultipliers, Accessed: 2018-08-15.
[5] W. Bo, Z. XueYing, C. Liang, Chinese Physics C Vol. 37 No.1 (2013) 010201

Acknowledgements

This work is partially supported by the Stewardship Science Academic Alliance through the Centaur Center of Excellence under Grant No. NA0003841.